Turbulence, Heat and Mass Transfer 4, pp. 689-696
K. Hanjalić, Y. Nagano and M. Tummers (Editors)

Hybrid RANS/LES employing Interface Condition with Turbulent Structure

S. Dahlström and L. Davidson

Department of Thermo and Fluid Dynamics, Chalmers University of Technology, SE-412 96 Göteborg, Sweden

Abstract — This paper deals with the use of a hybrid RANS/LES method. This approach has been applied on the flow in an asymmetric plane diffuser at a Reynolds number of 18000 based on the inlet bulk velocity and the inlet channel height. In the hybrid approach, a one-equation turbulence model is used in the near-wall region. At a certain distance from the wall, where the LES resolution is good, a switch to a one-equation SGS model is made. Turbulent structures are constructed from channel DNS data and used as an approximate condition at the interface between the LES and RANS regions. The RANS region is specified to be in a region with constant mass flow (i.e. the interface is located along a streamline). Computations with and without the interface condition and for various extents of the RANS region have been conducted and are presented in the paper. The standard hybrid RANS/LES approach produces poor results, whereas the interface condition improves the results considerably.

1. Introduction and Motivation

The idea with the hybrid RANS/LES approach is to use RANS in the near-wall region. This circumvents the resolution problem with wall-resolved large-eddy simulations, where the requirement on the resolution is based on wall units. Instead, in the hybrid approach, the requirement on the resolution is that it should be sufficiently fine in the region outside the near-wall region (in the off-near-wall region). This is the region where LES is applied and the requirement can be expressed in outer length scales, which can e.g. be related to the boundary layer thickness or the height of a separation region. In the diffuser case studied in this paper it could be based on the increasingly higher diffuser height. In the RANS region it should be assured that the RANS resolution is wall resolved (i.e. $y_1^+ < 1$). The amount of nodes saved are huge compared to wall-resolved large-eddy simulations, especially when aiming at solving for high-Reynolds number flows.

What are the benefits of using LES in the off-near-wall region? This was investigated (without any special near-wall treatment) in the flow around the Aerospatiale A-profile [1]. In this flow the treatment of the laminar region and the transition is probably more important than the near-wall modelling. It seems that the more complex the outer flow structures are, the more beneficial is LES. The near-wall structures play a less dominant role compared to the outer flow structures. An example, which has been successful, is the DES approach for massively separated flows [2–4].

However it is evident that in order to investigate the benefits of using LES in the off-near-wall region for this diffuser case the near-wall region must be modelled. In channel flows the near-wall structures play a dominant role and coarse LES fails to predict this seemingly simple flow. Also the standard hybrid RANS/LES approach does not produce good results [5]. An additional condition seems to be necessary at the interface between the RANS and LES region. In this paper this new interface condition is described and results from this approach are presented.

2. Governing Equations & Modelling Issues

Filtering or time averaging (the bar means filtering in the LES region and time averaging in the RANS region) of the incompressible continuity and momentum equations results in

$$\frac{\partial \overline{u}_i}{\partial x_i} = 0 \tag{1}$$

$$\frac{\partial \overline{u}_i}{\partial t} + \frac{\partial}{\partial x_j}(\overline{u}_i \overline{u}_j) = -\frac{1}{\rho}\frac{\partial \overline{p}}{\partial x_i} + \frac{\partial}{\partial x_j}\left[\nu \frac{\partial \overline{u}_i}{\partial x_j} - \tau_{ij}\right] \tag{2}$$

$$\tau_{ij} = \overline{u_i u_j} - \overline{u}_i \overline{u}_j \tag{3}$$

Here, τ_{ij} are the subgrid scale (SGS) or turbulence stresses. In LES they are the contribution of the small scales, the unresolved stresses. In RANS they are the contribution of all turbulence. In either case they are unknown and need to be modelled, here using the eddy-viscosity hypothesis:

$$\tau_{ij} - \frac{1}{3}\delta_{ij}\tau_{kk} = -2\nu_T \overline{S}_{ij} \tag{4}$$

Here, $\overline{S}_{ij} = \frac{1}{2}\left(\frac{\partial \overline{u}_i}{dx_j} + \frac{\partial \overline{u}_j}{dx_i}\right)$ is the strain rate.

The transport equation for the kinetic energy reads:

$$\frac{\partial k_T}{\partial t} + \frac{\partial}{\partial x_j}(\bar{u}_j k_T) = \frac{\partial}{\partial x_j}\left[(\nu + \nu_T)\frac{\partial k_T}{\partial x_j}\right] + P_k - C_\varepsilon \frac{k_T^{3/2}}{\ell_\varepsilon} \tag{5}$$

$$P_k = 2\nu_T \bar{S}_{ij}\bar{S}_{ij},\ \nu_T = C_k \ell_k k_T^{1/2} \tag{6}$$

	Chen and Patel	Yoshizawa [6]
C_ε	1	1.05
C_k	0.09	0.07
ℓ_ε	$2.495 \cdot y(1 - e^{-0.2y\sqrt{k}/\nu})$	Δ
ℓ_k	$2.495 \cdot y(1 - e^{-0.0143y\sqrt{k}/\nu})$	Δ

Table 1: The constants and length scales in the one-equation models.

The one-equation model used in the present computations is based on the one-equation SGS model by Yoshizawa [7] and the one-equation turbulence model by Chen and Patel [8]. In the LES region it models the kinetic energy of the unresolved stresses ($k_T = k_{sgs}$) and in the RANS region it is a model for the turbulent kinetic energy ($k_T = k$). The model constants and length scales are summarised in Table 1. In the LES region the filter width, Δ, is set to the third root of the finite-volume cell ($\Delta = (\Delta x \Delta y \Delta z)^{1/3}$).

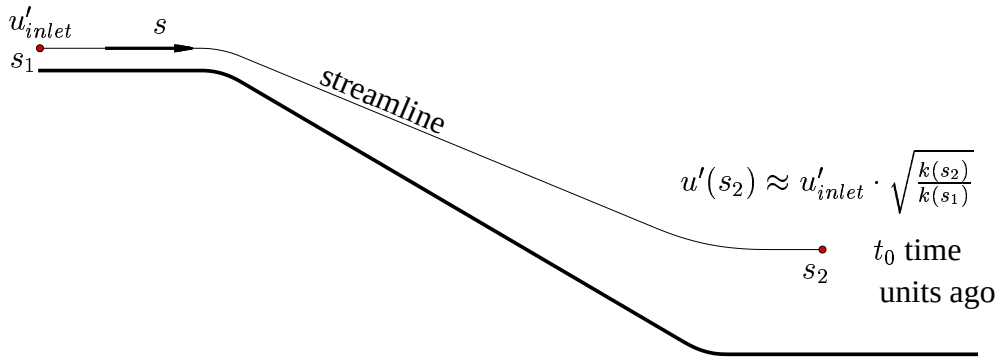

Figure 1: Interface condition using Taylor's hypothesis.

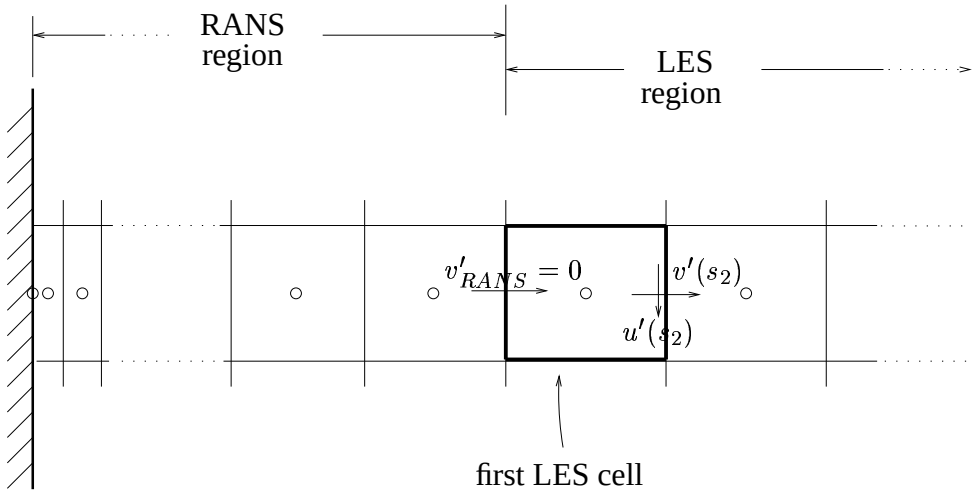

Figure 2: Interface condition implemented at the first LES cell using the comstructed velocity fluctuations, u' and v' (w' not shown), and $v'_{RANS} = 0$.

2.1. Interface condition

Instantaneous DNS data from a channel computation at $Re_\tau = 500$ are used as inlet boundary conditions. The instantaneous DNS data, at a prescribed distance from the wall, are transformed along a matching plane at each time step using Taylor's hypothesis or the assumption of "frozen turbulence". We imagine that the DNS turbulence is frozen and just convected downstream (see Fig. 1). At each point, s_2, at the matching plane, we can compute the travelling time, t_0, it takes for the inlet data (at point s_1) to reach point s_2, as

$$t_0 = -\int_{s_1}^{s_2} \frac{ds}{u_s(s)}, \tag{7}$$

where u_s is the velocity along the streamline. The level of the turbulence is modified by scaling it with the kinetic energy at the point, $k(s_2)$, (from the one-equation model) and the inlet kinetic energy, $k(s_1)$, (from the DNS data):

$$u'(s_2, z, t) = u'(s_1, z, t_0) \cdot \sqrt{\frac{k(s_2)}{k(s_1)}} \tag{8}$$

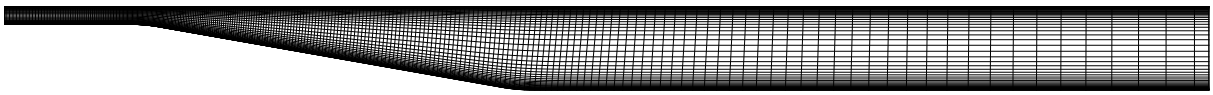

Figure 3: The diffuser mesh ($258 \times 66 \times 24$ nodes).

This is computed in the same way for the fluctuations in the other directions (v' and w'). In this way approximate turbulent structures are constructed at the matching plane. These structures are implemented in the code at the first LES cell imposing that the resolved stresses are zero in the RANS region (see Fig. 2). For the interface close to the lower wall the source added to the momentum equations in the LES cell adjacent to the matching plane is

$$-u_i'(s_2)v'(s_2)A_s, \tag{9}$$

where index i denotes x_i direction and A_s denotes the area of the LES cell facing the matching plane. This source corresponds to adding the term $-\partial\langle u_i'v'\rangle/\partial n$ to the differential form of the momentum equations (Eq. 2). Here n is the coordinate from the wall into the flow.

3. Computational Setup

Based on the inlet channel height, H, and the bulk velocity, U_b, the Reynolds number is 18000. The outlet channel has a height of $4.7H$. At $x/H = 0$ the inclined wall starts with a slope of approximately 10° and ends 21 channel heights downstream. More details about the asymmetric plane diffuser case can e.g. be found in Ref. [9]. The experiments have been conducted by Buice and Eaton [10], where extensive care has been taken to assure the two-dimensionality of the flow. In these experiments the Reynolds number is 20000, based on the centerline velocity, U_c, resulting in a slightly lower Reynolds number in the experiments compared to the computational setup. In the experiments $Re_b = 17544$, since $U_c = 1.14U_b$.

Figure 3 shows the mesh, which consists of 258 nodes in the streamwise direction, 66 in the wall-normal direction and 24 nodes in the spanwise direction. The grid size, Δz, is set to $0.184H$ and thus the extent in this direction, L_z, is equal to $4.0H$. The wall distance to the first node, y_1^+, is less than 1. The inlet is located at $x = -7.9H$ and the outlet at $x = 60H$. Figure 4 shows the resolution along the top wall of the diffuser (it is finer on the lower wall). The resolution is too coarse for a wall-resolved simulation as is seen in the wall-unit based plot. The resolution expressed in the half height of the diffuser is also shown in Fig. 4.

An incompressible, finite volume code is used [11]. For space discretisation, central differencing is used for all terms. The Crank-Nicolson scheme is used for time discretisation. The numerical procedure is based on an implicit, fractional step technique with a multigrid pressure Poisson solver and a non-staggered grid arrangement [12].

The time step is set to $\Delta t = 0.0441H/U_b$ (giving a maximum CFL-number of approximately one). The time averaging is started after one flow-through time and the data is then collected for another 5 flow-through times. At the outlet a convective boundary condition is used for the velocities. Instantaneous DNS data from a channel computation at $Re_\tau = 500$ is used as inlet boundary condition.

4. Results

Results from four computations are presented in this paper. Three of them are hybrid RANS/LESs with different extents of the RANS region. The interfaces are located at $y_{ml}^+ \approx 43$, $y_{ml}^+ \approx 60$

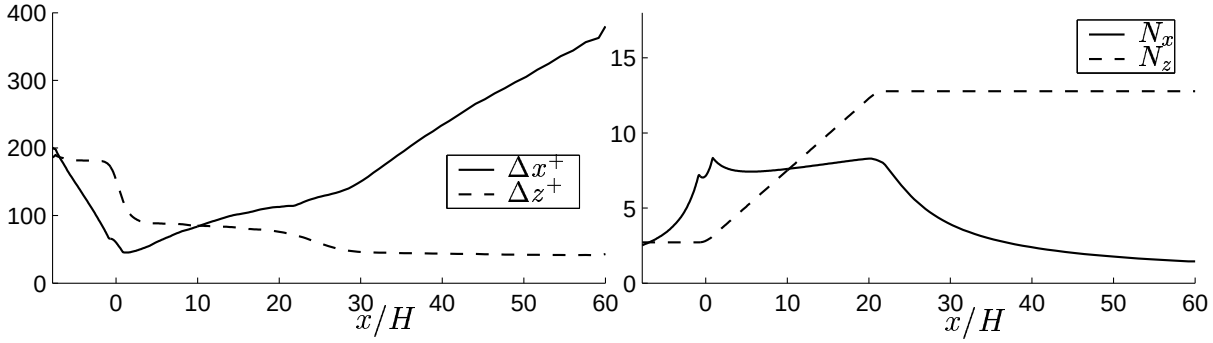

Figure 4: Resolution along the diffuser based on wall units and based on outer length scales. N_x and N_z are the amount of nodes per half height of the diffuser in the streamwise and spanwise direction, respectively.

and $y^+_{ml} \approx 82$. These values are at the inlet channel. Downstream, the RANS region is within a constant mass flow (so that the streamwise mass flow in the RANS region is constant for all x). These simulations are compared to the best RANS computation presented in Ref. [5]. Also simulations without the interface condition have been conducted with the matching lines at the locations above. However these simulations are not shown here. They produce poor results, e.g. the separation is not predicted.

The results are shown in Figs. 5-9. Streamlines are shown in Fig. 5 for the hybrid RANS/LES approach and the figure shows that the simulation is instationary in the LES region.

The pressure and skin friction coefficients are shown in Fig. 6. The skin friction coefficient is reasonably well predicted on the bottom wall for the hybrid RANS/LES computations with $y^+_{ml} \approx 43$ and $y^+_{ml} \approx 60$. The level for the pressure coefficient is too high in the diffuser for the simulations with $y^+_{ml} \approx 60$ and $y^+_{ml} \approx 82$.

In Fig. 7 velocity profiles are shown and compared to experiments. In the RANS computation (the thick lines) we get good results in the inlet channel and in the inclined wall region. Downstream of the inclined wall the mechanism of the reattachment is poorly captured (it is far too slow), the separation bubble being too long and the recovery length much too long. This is a usual problem for RANS models: to have a too slow redevelopment of the boundary layer downstream of the reattachment.

Two of the hybrid RANS/LESs gives good results all along the diffuser and the length of the separation bubble is close to the length measured in the experiments. In the experiments the reattachment location is at approximately $29H$ (the separation is between $x/H = 6.5$ and $x/H = 7$). Although channel flow simulations produced good results at $y^+_{ml} \approx 82$ [5], the simulation in the diffuser produces poor results and apparently the matching line is too far from the wall.

The resolved normal stresses in the streamwise direction are shown in Fig. 8. The stresses are low in the RANS region for the hybrid approach, especially in the separated region. The eddy viscosities are shown in Fig. 9, note how the RANS region extends far from the wall in the separated-flow region because of the mass flow condition for the matching line. The idea with hybrid RANS/LES is illustrated in Fig. 9: when reaching the LES region, the eddy viscosity decreases significantly and the resolved stresses increase.

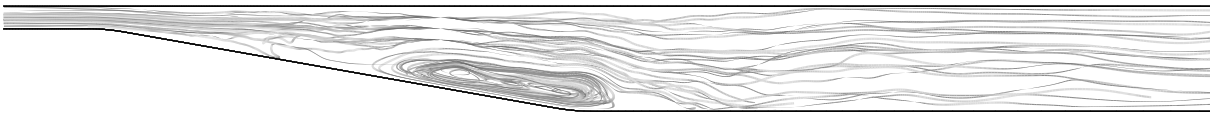

Figure 5: Instantaneous streamlines, from the $y^+_{ml} \approx 43$-case.

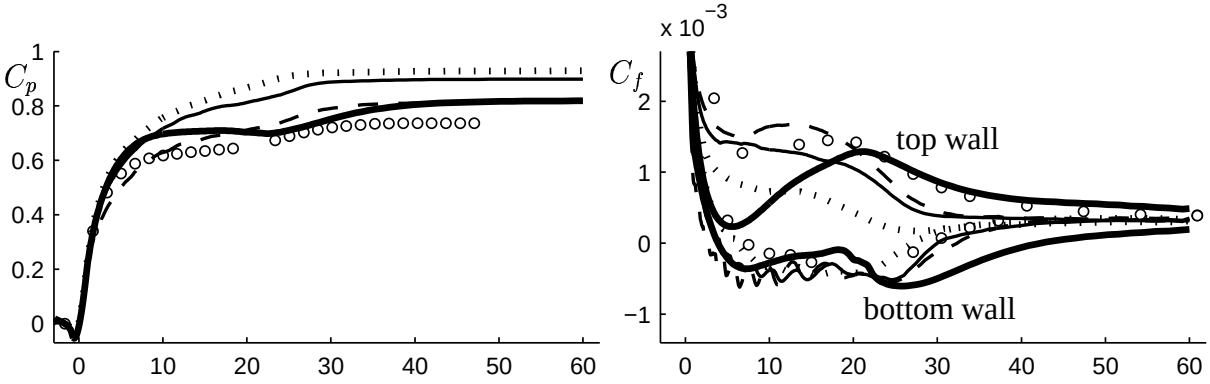

Figure 6: Pressure coefficients on the bottom wall and skin friction coefficients. Dashed line: $y^+_{ml} \approx 43$-case; thin solid line: $y^+_{ml} \approx 60$-case; dotted line: $y^+_{ml} \approx 82$-case; thick solid line: RANS computation.

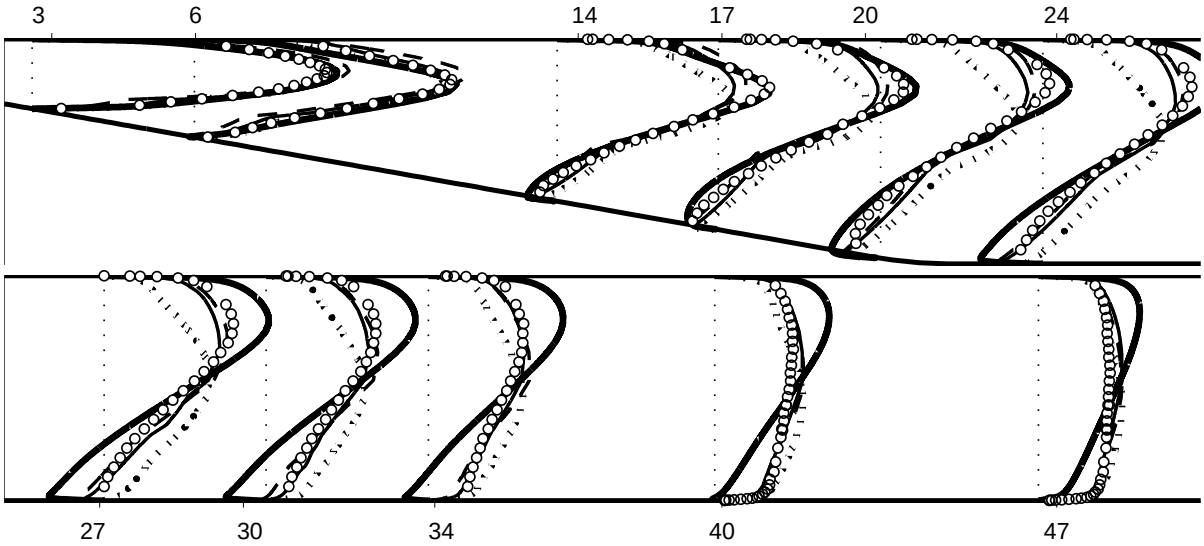

Figure 7: Velocities, $\langle \overline{U} \rangle$. Dashed line: $y^+_{ml} \approx 43$-case; thin solid line: $y^+_{ml} \approx 60$-case; dotted line: $y^+_{ml} \approx 82$-case; thick solid line: RANS computation.

5. Conclusions & Ongoing Work

The RANS computation shows a too slow recovery of the outlet channel boundary layer. In the hybrid simulations the redevelopment of the boundary layer in the outlet channel is better and the mechanism of the reattachment is better captured. The results are promising showing good results for a RANS region extending up to $y^+_{ml} \approx 60$ at the inlet channel.

In future work still more tests will be conducted on the diffuser and the approach will also be applied on the fbw around the Aerospatiale A-profile. In case of external fbw with massive

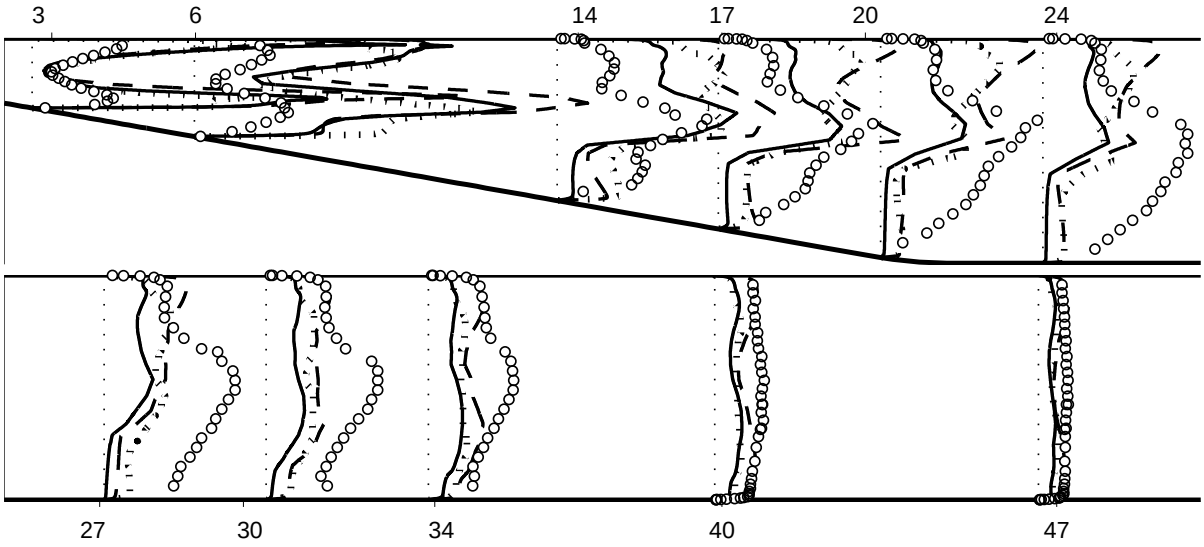

Figure 8: Resolved $\langle\overline{uu}\rangle$ stresses. Dashed line: $y^+_{ml} \approx 43$-case; thin solid line: $y^+_{ml} \approx 60$-case; dotted line: $y^+_{ml} \approx 82$-case.

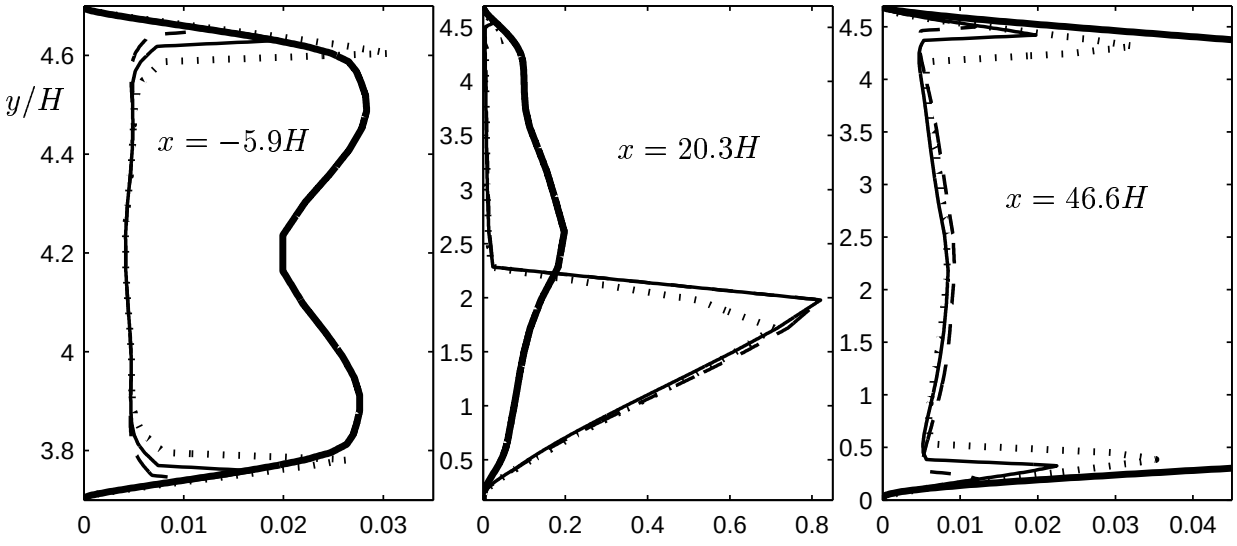

Figure 9: Eddy viscosities. Dashed line: $y^+_{ml} \approx 43$-case; thin solid line: $y^+_{ml} \approx 60$-case; dotted line: $y^+_{ml} \approx 82$-case; thick solid line: RANS computation. Note that the scaling differs in the three plots.

separation the wall distance to the interface must be limited.

Acknowledgements

This work was financed by the FLOMANIA project (Flow Physics Modelling - An Integrated Approach) and is a collaboration between Alenia, AEA, Bombardier, Dassault, EADS-CASA, EADS-Military Aircraft, EDF, NUMECA, DLR, FOI, IMFT, ONERA, Chalmers University, Imperial College, TU Berlin, UMIST and St. Petersburg State University. The project is funded by the European Union and administrated by the CEC, Research Directorate-General, Growth Programme, under Contract No. G4RD-CT2001-00613.

References

1. S. Dahlström and L. Davidson. Large eddy simulation of the flow around an airfoil. 39th Aerospace Sciences Meeting, AIAA Paper 2001-0425, Reno, 2001.
2. P.R. Spalart, W-H. Jou, M. Strelets, and S.R. Allmaras. Comments on the feasibility of LES for wings, and on a hybrid RANS/LES approach. 1st AFOSR Int. Conf. on DNS/LES, Aug. 4-8, 1997, Ruston, LA. In *Advances in DNS/LES, C. Liu & Z. Liu Eds., Greyden Press, Columbus, OH*, 1997.
3. M. Shur, P. R. Spalart, M. Strelets, and A. Travin. Detached-eddy simulation of an airfoil at high angle of attack. In W. Rodi and D. Laurence, editors, *Engineering Turbulence Modelling and Experiments 4*, pages 669–678. Elsevier Science, 1999.
4. M. Strelets. Detached eddy simulation of massively separated flows. 39th Aerospace Sciences Meeting, AIAA Paper 2001-0879, Reno, 2001.
5. S. Dahlström. *Large Eddy Simulation of the Flow around a High-Lift Airfoil*. PhD thesis, Dept. of Thermo and Fluid Dynamics, Chalmers University of Technology, Gothenburg, 2003.
6. C. Fureby. Large eddy simulation of rearward-facing step flow. *AIAA Journal*, 37(11):1401–1410, 1999.
7. A. Yoshizawa. Statistical theory for compressible shear flows with the application of subgrid modelling. *Physics of Fluids A*, 29:2152–2163, 1986.
8. H.C. Chen and V.C. Patel. Near-wall turbulence models for complex flows including separation. *AIAA Journal*, 26:641–648, 1988.
9. 8th ERCOFTAC/IAHR/COST workshop on refined turbulence modelling. In *June 17-18, Helsinki University of Technology, Helsinki, Finland*, 1999.
10. C. U. Buice and J. K. Eaton. Experimental investigation of flow through an asymmetric plane diffuser. Report TSD-107, Thermosciences Division, Department of Mechanical Engineering, Stanford University, Stanford, CA, USA, 1997.
11. L. Davidson. Hybrid LES-RANS: A combination of a one-equation SGS model and a $k-\omega$ model for predicting recirculating flows. In *ECCOMAS CFD Conference*, Swansea, U.K., 2001.
12. P. Emvin. *The Full Multigrid Method Applied to Turbulent Flow in Ventilated Enclosures Using Structured and Unstructured Grids*. PhD thesis, Dept. of Thermo and Fluid Dynamics, Chalmers University of Technology, Gothenburg, 1997.